Catalysis
Science &
Technology

Accepted Manuscript

This article can be cited before page numbers have been issued, to do this please use: R. K. Sharma, M. Yadav, R. Gaur, Y. Monga and A. Adholeya, *Catal. Sci. Technol.*, 2015, DOI: 10.1039/C4CY01736F.

ROYAL SOCIETY
OF CHEMISTRY

www.rsc.org/catalysis

Catalysis Science & Technology

Dynamic Article Links ►
View Article Online
DOI: 10.1039/C4CY01736F

Cite this: DOI: 10.1039/c0xx00000x

www.rsc.org/xxxxxx

ARTICLE TYPE

Magnetically retrievable silica based Nickel nanocatalyst for Suzuki-Miyaura Cross coupling reaction

Rakesh Kumar Sharma,*[a] Manavi Yadav,[a] Rashmi Gaur,[a] Yukti Monga[a] and Alok Adholeya[b]

Received (in XXX, XXX) Xth XXXXXXXXX 20XX, Accepted Xth XXXXXXXXX 20XX
DOI: 10.1039/b000000x

A new magnetically recoverable silica based nickel nanocatalyst was synthesized, characterized and applied for the first time as a catalyst in Suzuki-Miyaura cross coupling reaction. Excellent catalytic activity, ease of recovery and reusability upto six cycles without appreciable loss of performance, makes the present protocol beneficial from industrial and environmental viewpoint.

1. Introduction

Over the last few decades the quest for the most economic ways in the formation of C-C bond has become a matter of increasing importance among the industrial and academic research units.[1] This paradigm construction of biaryl moiety enables facile preparation of numerous structurally diverse and complex molecules essential for the development of modern pharmaceuticals, agrochemicals and organic materials.[2] Owing to its significant applications, transition metal-catalyzed cross-coupling reactions have witnessed tremendous advances for selective C-C bond formation.[3] Among them, palladium (Pd) has been the first choice and is still one of the most frequently investigated metals for cross-coupling reactions.[4] However, due to its robust demand and limited resources, dispersion of Pd from the environment has raised a key concern regarding its availability in near future.[5] Therefore, there is an urgent need to explore other available and cost-effective metal catalyst. In this context, a recent surge of interest is growing up for more abundant first-row transition-metal based catalysts.[6] As a promising solution to this issue, nickel (Ni) catalysis has emerged as a viable alternative to Pd catalyzed cross-coupling reactions.[7] Also, being comparatively smaller in size, it has the ability to undergo the oxidative addition step with aryl halides much more readily than Pd counterparts. Indeed, as compared to Pd, Ni-based catalysts are more specific and versatile due to their unique reactivity and catalytic behavior and have been continuously employed as powerful catalysts for the construction of a wide variety of C–C, C–N, and C–P bond forming reactions.[8]

Despite the substantial progress made towards the development of Ni-based catalytic systems for various cross-coupling reactions, a common feature involves homogeneous catalysis.[9] Arguably the greatest barrier to the wider adoption of homogeneous catalysis is the difficulty in separation of the metal from the product stream and the ability to recover and reuse the catalyst. To circumvent the aforementioned drawbacks, heterogenization of the existing homogeneous catalysts has contributed greatly as an attractive solution, as the heterogeneous catalytic systems can be efficiently re-used whilst keeping the inherent activity of the catalytic centre.[10]

To date, various attempts have been made for the development of Ni- based heterogeneous catalyst for Suzuki reaction.[11] In 2000, Lipshutz *et al.* reported Ni immobilized on charcoal as a heterogeneous catalyst for Suzuki reaction.[11a] Later, they found enhanced efficiency for Suzuki, when Ni was anchored on graphite.[11b] Further, Wang *et al.* reported Ni-metal colloid using TBAB as a stabilizer for cross-coupling reactions.[11c] Unfortunately, these methodologies suffered from several drawbacks such as harsh reaction conditions, high temperature, longer reaction time, use of toxic reducing agents, and had both storage and handling difficulties. However, in recent years, there are some reports on the use of Ni nanoparticles as heterogeneous catalyst for the Suzuki coupling reaction, but these catalysts faced numerous limitations including low catalytic efficiency, lack of stability, metal leaching issues and little reusability.[12]

Recently, magnetic nanoparticles (MNPs) have engrossed immense attention as sustainable alternatives to conventional heterogeneous catalytic support.[13] Besides, preserving all the desirable attributes of both homogeneous and heterogeneous catalysis, they offer an added advantage of facile separation by magnetic forces, and paves the way for tedious procedures of catalyst filtration or centrifugation, after completion of the reaction. However, they have a tendency to aggregate, which is eliminated by silica coating. Apart from screening the dipolar attraction between MNPs, silica shell also imparts various desirable properties to it such as, excellent thermal stability, chemical inertness and ease of succedent functionalization.[14]

As a part of our ongoing research work in the development of green and sustainable protocols.[15] We herein describe a first report wherein magnificent properties of silica are incorporated

View Article Online
DOI: 10.1039/C4CY01736F

with the magnetic properties of nanoparticles and catalytic properties of nickel for performing Suzuki-Miyaura cross-coupling reaction. This system is of interest as it possesses excellent stability, good activity, and is more cost-effective than other previously reported catalysts.

2. Experimental

2.1 General

TEOS (tetraethoxyorthosilicate) was procured from Sigma Aldrich and 3-Aminopropyl-triethoxysilane (APTES) was obtained from Fluka. Ferric sulphate and ferrous sulphate were purchased from Sisco Research Laboratory (SRL). Nickel (II) chloride hexahydrate, Ethanol, 1, 4-Dioxane and Ethyl acetate (EtOAc) were purchased from Merck. Double deionized water was used throughout the study. All the other reagents used were of analytical grade and commercially available.

The catalyst was analyzed through different techniques, which ensured a complete composition, morphology, functionalization, magnetization and size characterization. X-ray diffraction (XRD) was performed using a D8 Discover Bruker AXS, (Karlsruhe, Bundesland, Germany) diffractometer equipped with Cu/Kα radiation at a scanning rate of 4°/min in the 2θ range of 5–80° (λ = 0.15406 nm, 40 kV, 40 mA). The morphology and uniformity of nanoparticles were investigated by FEI TECHNAI G2 T20, Transmission Electron Microscope operated at 200 kV by dispersing sample on a copper grid coated with an amorphous carbon film and the “ImageJ” software was used for image processing and analysis.
The chemical composition of the particles was determined by X-ray energy-disperse spectroscopy (EDS) by using an Ametek EDAX system. SEM was performed using Carl Zeiss India, Scanning Electron Microscope for the characterization of structural properties of prepared nanocomposites. Sample preparation was done by dispersing nanoparticles in ethanol and drop casting the sample on metal stub covered with an aluminium tape. Sample was then dried using pressurized air and sputter-coated with a 3 nm Au-Pd layer using mini sputter coater SC7620 of Qourum technologies under vacuum and finally the sample was subjected to scanning electron microscope.
Magnetization measurements M (T, H) were performed by using EV-9, Microsense, ADE vibrating sample magnetometer. The Fourier transform infrared spectra (FT-IR) of nanoparticles were collected using Perkin-Elmer Spectrum 2000. Digestions were performed in Anton Paar multiwave 3000 microwave reaction system equipped with temperature and pressure sensor. The amount of nickel in the catalyst and in the supernatant was estimated by Atomic absorption spectroscopy (AAS) on Analytik Jenas ZEEnit700P Atomic Absorption Spectrometer using an acetylene flame. The derived products were analyzed and confirmed by using Agilent gas chromatography (6850 GC) with a HP-5MS 5% phenyl methyl siloxane capillary column (30.0 m × 0.25 mm × 0.25 mm) and a quadrupole mass filter equipped 5975 mass selective detector (MSD) using helium as a carrier gas. XPS studies were also performed to determine the oxidation state of Nickel present in the synthesized catalyst.

2.2 Catalyst preparation

The first step towards the synthesis of desired catalyst is the preparation of magnetic nanoparticles by co-precipitation technique **(Scheme 1)**.[16] Considering the aggregation tendency of naked magnetic nanoparticles (MNPs), they were further coated with silica (SMNPs), which not only solves the problem of aggregation but also provides suitable sites for surface functionalization. Finally, NH_2 linker (APTES) was covalently coupled to the hydroxyl group present on the surface of the magnetic silica nanoparticles for the grafting of other substrates. APTES functionalized silica encapsulated magnetic nanoparticles (ASMNPs) were further reacted with ligand, thiophene-2 carboxaldehyde (TC) and the resulting NPs were metallated with nickel chloride hexahydrate ($NiCl_2.6H_2O$) to produce the final catalyst (Ni-TC@ASMNPs).

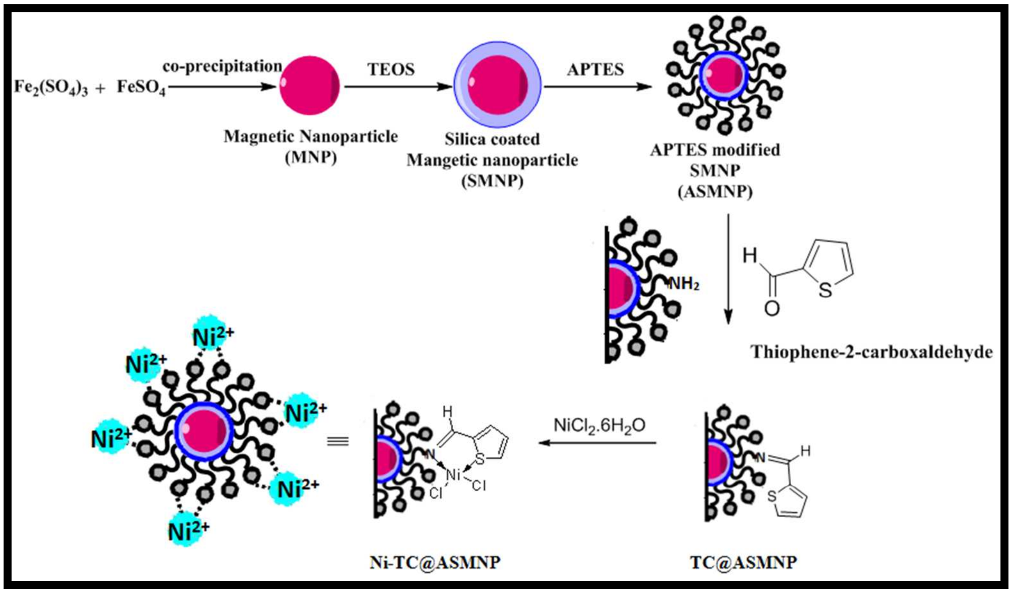

Scheme 1 A schematic illustration for the formation of Ni-TC@ASMNP nanocatalyst

Catalysis
Science & Technology

Catalysis Science & Technology

Dynamic Article Links ►
View Article Online
DOI: 10.1039/C4CY01736F

Cite this: DOI: 10.1039/c0xx00000x

www.rsc.org/xxxxxx

ARTICLE TYPE

2.2.1 Synthesis of APTES functionalized silica coated magnetic nanoparticles

For this purpose, 6.0 g of $Fe_2(SO_4)_3$ and 4.2 g of $FeSO_4$ was dissolved in 250 mL water and was stirred at 60 °C to give a yellowish-orange solution. To this, 15 mL of 25% NH_4OH solution was added with vigorous stirring and colour of the bulk solution turned black. Stirring was continued for another half an hour and the precipitated MNPs were separated using external magnet and washed several times with deionized water and ethanol. Silica coating over these MNPs was achieved via sol-gel approach.[15b] Dispersed solution of activated 5.0 g of MNPs with 0.1 M HCl (2.2 mL) in 200 ml ethanol and 50 mL water was obtained under sonication. Then, 5 mL of 25% NH_4OH solution was added to the suspension at room temperature followed by the addition of 1mL of TEOS and the solution was kept for stirring at 60 °C for 6 h. The obtained SMNPs were magnetically separated, washed with ethanol and dried under vacuum. The obtained SMNPs were further functionalized using APTES to afford ASMNPs. This was done by adding APTES to the dispersed solution of 0.1 g SMNP in 100 mL ethanol, under sonication and the resulting mixture was stirred at 50 °C for 6 h.

2.2.2 Synthesis of Ni-TC@ASMNP

For covalent grafting of the ligand on ASMNPs, 1g of ASMNP was refluxed with TC in dried methanol along with molecular sieves at 70 °C for 3 h. The obtained product was washed with methanol and dried under vacuum. Finally, 1 g of grafted TC@ASMNPs was stirred with a solution of 4 mmol of $NiCl_2.6H_20$ in methanol for 3 h. The resulted Ni-TC@ASMNPs were separated magnetically and thoroughly washed with deionized water and dried under vacuum.

2.3 Reaction procedure for Suzuki-Miyaura cross coupling reaction

15 mg of Ni-TC@ASMNP catalyst was taken in an oven dried round bottom flask, and to this, PPh_3 (20 mol%), aryl halide (0.5 mmol) and phenyboronic acid (0.6 mmol) were added. After this K_3PO_4 (0.75 mmol) was added, followed by the addition of 1 mL dioxane. The reaction mixture was kept under N_2 atmosphere and was stirred at 100 °C till the completion of the reaction **(Scheme 2)**. The catalyst was recovered with permanent magnet. Reaction was monitored using thin layer chromatography and the products were extracted using ethyl acetate, dried over sodium sulphate, concentrated under reduced pressure, and analyzed by GC-MS.

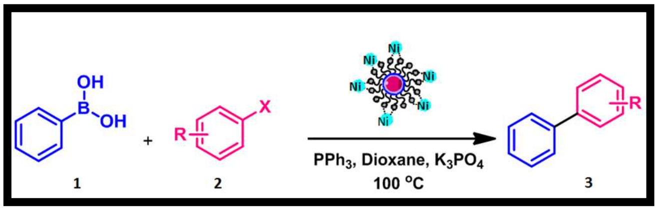

Scheme 2 Ni-TC@ASMNP nanocatalyst catalyzed Suzuki-Miyaura cross-coupling reaction

3. Results and Discussion

3.1 Characterizations

3.1.1 Fourier-transform Infrared Spectroscopy

Due to the superparamagnetic nature of magnetic nanoparticle, NMR technique could not be used for the confirmation of its surface modification. Instead, Fourier transform Infrared spectroscopy was employed to demonstrate the functionalization of the synthesized composites in the range of 4000–400 cm^{-1}. **Fig. 1a** exhibits the characteristic band at 586 cm^{-1} due to the vibration of the Fe–O bond in the tetrahedral site of bare magnetic nanoparticles and splitting corresponds to the Fe–O bond of bulk magnetite.[17a] The broad band at 3367 cm^{-1} is assigned to the O–H stretching vibration arising from adsorbed water. The coating of silane matrix onto the surface of MNPs was confirmed by two new bands at 1088 cm^{-1} and 802 cm^{-1} which are ascribed to the symmetrical and asymmetrical vibrations of the Si–O–Si bonds **(Fig. 1b)**.[17b] Also, the stretching absorption of Fe–O at 586 cm^{-1} shifts to high wave number of 614 cm^{-1} after coating with silica. Moreover, a significant reduction in the spectral intensity was observed, while moving from MNPs to SMNPs. Thus, it was clearly concluded that MNP was successfully coated with a silica layer. In the spectra of ASMNPs **(Fig. 1c)**, the appearance of the two broad bands at 3422 and 1633 cm^{-1} were due to the N–H stretching and NH_2 bending vibrations of free NH_2 group, respectively.[17c] After Schiff's condensation **(Fig. 1d)**, a characteristic band of the imine group (C=N) appears at 1651 cm^{-1},[17d] which confirms that thiophene-2-carboxaldehyde is chemically bonded to the surface of functionalized silica. Furthermore, on metallation with Nickel chloride, it is observed that the prominent absorption peak of C=N at 1651 cm^{-1} is shifted to a lower wave number 1643 cm^{-1} in **Fig. 1e**, indicating strong metal-ligand interaction (See **ESI-** S1).

View Article Online
DOI: 10.1039/C4CY01736F

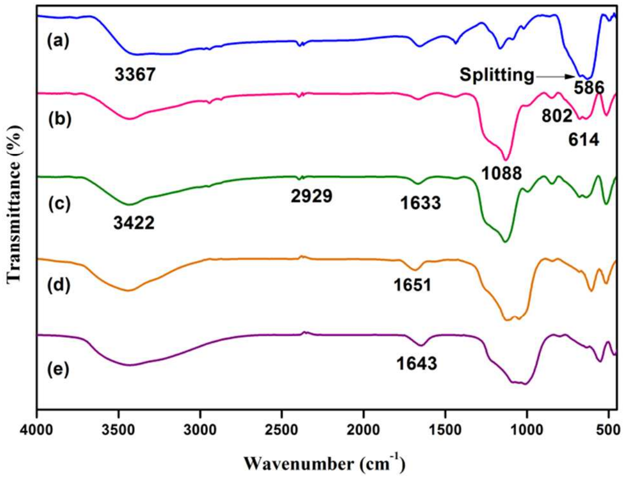

Fig. 1 FT-IR spectra of (a) MNP, (b) SMNP, (c) ASMNP, (d) TC@ASMNP and (e) Ni-TC@ASMNP

3.1.2 X-Ray Diffraction studies

In order to investigate phase, purity and crystalline nature of synthesized nanoparticles (MNP, SMNP, Ni-TC@ASMNP) and confirm their structural modification, powder X-ray diffraction (XRD) studies were conducted. XRD of the bare MNPs in **Fig. 2a** displayed patterns consistent with standard XRD data of the Joint Committee on Powder Diffraction Standards (JCPDS) card number (19-0629) for Fe_3O_4 crystal. All the observed diffraction peaks were indexed to the inverse cubic spinel structure of Fe_3O_4, revealing the high phase purity and high crystallinity of the Fe_3O_4 nanocore. As depicted from the diffractogram, the patterns indicate a crystallized structure at 2θ: 16.181°, 30.366 °, 35.663 °, 43.024 °, 57.299 °, and 62.865 °, which are assigned to the (111), (2 2 0), (3 1 1), (4 0 0), (5 1 1) and (4 4 0) crystallographic faces of magnetite.[18a] The Debye–Scherrer equation (Dhkl 1/4kl/β cos θ) was used to estimate the mean crystallite size from the XRD patterns, where D is the size of the axis parallel to the (hkl) plane, k is a constant with a typical value of 0.89 for spherical particles, l is the wavelength of radiation, β is the full width at half maximum (FWHM) in radians, and θ is the position of the diffraction peak maximum. Here, the average crystallite size of Fe_3O_4 nanoparticles was calculated to be 11.4 nm by measuring the (3 1 1) peak widths of the XRD lines. Same peaks were observed in the silica-coated nanoparticle XRD patterns in **Fig. 2b**, indicating retention of the crystalline spinel ferrite core structure during the silica-coating process. A weak broad hump appeared in the spectra of SMNP from $2\theta = 20^\circ$ to 30° which was consistent with the formation of amorphous silica phase around the magnetic core, owing to very small crystallite size (See **ESI-S2**).[18b] Other than this, no any substantial variation was observed in the rest of the XRD pattern of SMNP, revealing the preservation of the original crystallographic structural characteristic of magnetite (Fe_3O_4) even after the extreme chemical and physical conditions created during the silica coating process.

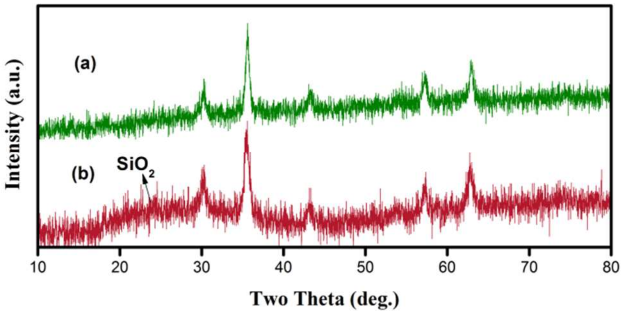

Fig. 2 XRD pattern of (a) MNPs and (b) SMNPs

3.1.3 SEM analysis

Fig. 3a and **b** represents the SEM images of bare magnetic nanoparticles and silica encapsulated magnetic nanoparticles, respectively. The smooth surface of magnetic core particles gets spongy due to uniform silica coating around the surface of MNPs. No separate aggregates of silica were found, thereby indicating that the silica coating has occurred only along the surface of MNPs. **Fig. 3c** shows the SEM image of the final catalyst Ni-TC@ASMNPs, which further confirms that the surface modification procedures did not affect the morphology of the magnetite cores. **Fig 3d** displays the SEM image of recovered catalyst after the completion of reaction which indicates that the shape and morphology of the catalyst remains unchanged.

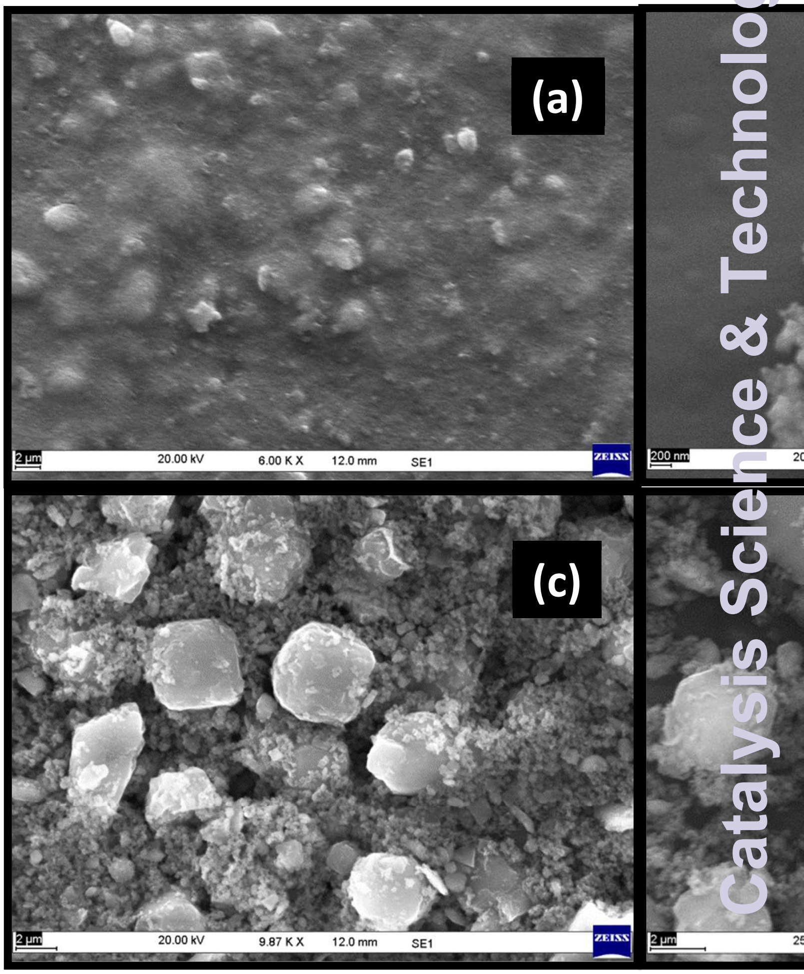

View Article Online
DOI: 10.1039/C4CY01736F

Fig. 3 SEM images of (a) MNPs, (b) SMNPs, (c) Ni-TC@ASMNPs and (d) Recovered Ni-TC@ASMNPs

3.1.4 Metal content determination and Oxidation state of Metal in catalyst

Energy dispersive X-ray Spectroscopy (EDS) displayed the elemental composition after the grafting reaction, verifying the presence of Ni, Fe and Si in the nanocatalyst (**Fig. 4**).The quantitative determination of the metal content was obtained by AAS analysis and was found to be 0.208 mmolg^{-1}.

In the XPS spectrum of the Ni-TC@ASMNPs, peaks were observed at higher binding energy (855.98 eV and 855.71 eV) confirming Ni^{2+} ion before and after catalysis. [19] (See **ESI**-S8, S9)

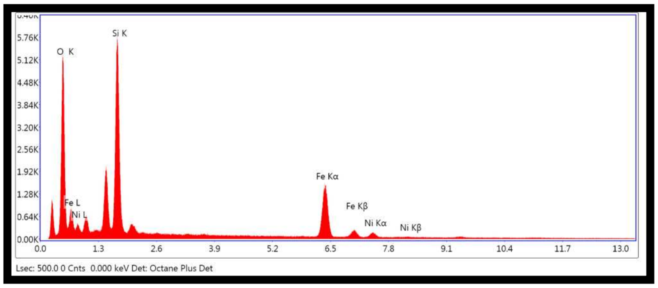

Fig. 4 EDS pattern of Ni-TC@ASMNPs

3.1.5 TEM analysis

The size and shape of synthesized nanoparticles were deduced from the TEM images. TEM micrographs provide clearer picture of the particle size and morphology of nanocomposites. The uncoated MNPs show slight agglomeration **(Fig. 5a)**, which exists due to the absence of surfactants and the lack of any repulsive forces between the magnetic nanoparticles.[20] Highly crystalline nature of nanocomposites is represented by the white spots and array of bright diffraction rings in the SAED pattern of nanoparticles **(Fig. 5b)**. From HRTEM image **(Fig. 5c)**, the average interplanar distance of MNPs was measured to be ~0.25 nm, which corresponds to (3 1 1) plane of inverse spinel structured Fe_3O_4. Moreover, **Fig. 5d** showed that the silica coating was almost homogeneous and a closer examination of the image reveals that the silica-coated magnetic nanoparticles display dark MNP cores due to their high density, surrounded by a lighter amorphous silica shell of about 4-5 nm thick. **Fig. 5e** depicts the size distribution histogram of about 100 colloidal aggregates of MNPs with maximum particle size in the range of 10-12 nm (See **ESI**-S3). The size estimated from TEM micrographs agrees well with the crystallite size estimated from XRD line profile fitting. TEM analysis of the nanoparticles indicated that both pure MNPs and SMNPs were quasi spherical in shape.

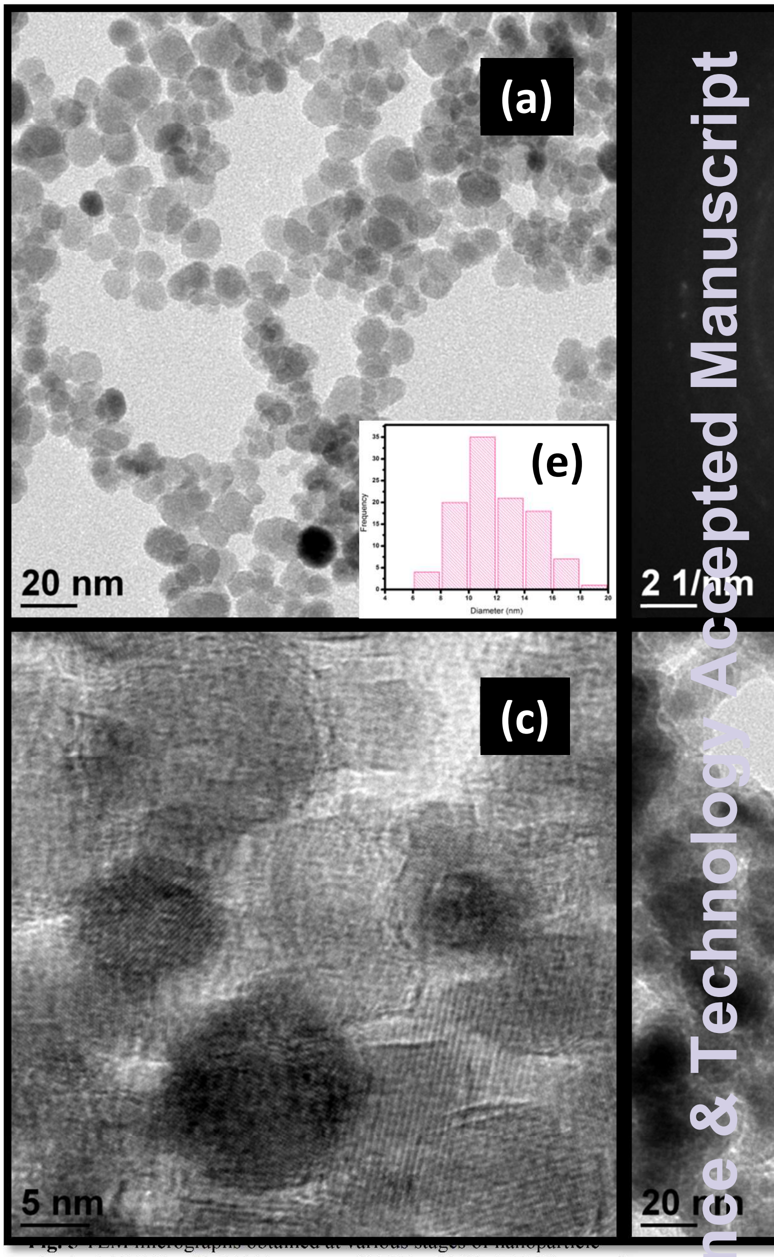

Fig. 5 TEM micrographs obtained at various stages of nanoparticle synthesis: (a) MNPs, (b) SAED pattern of MNPs, (c) HR-TEM image of MNP, (d) SMNPs and (e) inset: histogram illustrating size distribution of MNPs

3.1.6 VSM

The magnetization measurements of bare MNPs, SMNPs, ASMNPs and Ni-TC@ASMNPs were investigated at room temperature (298K) using vibration sample magnetometer (VSM) with the field sweeping from −20, 000 to 20,000 Oe. **Fig. 6** shows the magnetization curves of MNP, SMNP, ASMNP and Ni-TC@ASMNP. At the same field, the saturation magnetization value (Ms) for MNPs was found to be 58 emu/g, which is less than its bulk counterpart (90 emu/g).[21a] This decrease can be attributed to the nanosize of the obtained MNPs as the size of magnetic particles is directly proportional to its magnetization value. For SMNPs, ASMNPs and Ni-TC@ASMNPs, the

View Article Online
DOI: 10.1039/C4CY01736F

magnetization value gets further reduced to 42, 26 and 15 emu/g respectively, due to the contribution of the non-magnetic silica shell and functionalized groups on the surface of MNPs. Even though the Ms values of MNPs have evidently decreased, they could still be efficiently removed from solution media with a permanent magnet.[21b] The enlarged magnetization curve (**Fig. 6e**) for all three nanoparticles showed typical characteristic features of superparamagnetic behaviour i.e., zero coercivity and negligible remanence, by passing through the origin on M-H hysteresis. This also implies that magnetic materials can be aligned only under magnetic field and will not retain their residual magnetism once the field is removed, thereby making magnetic nanoparticles good candidate for catalytic support.

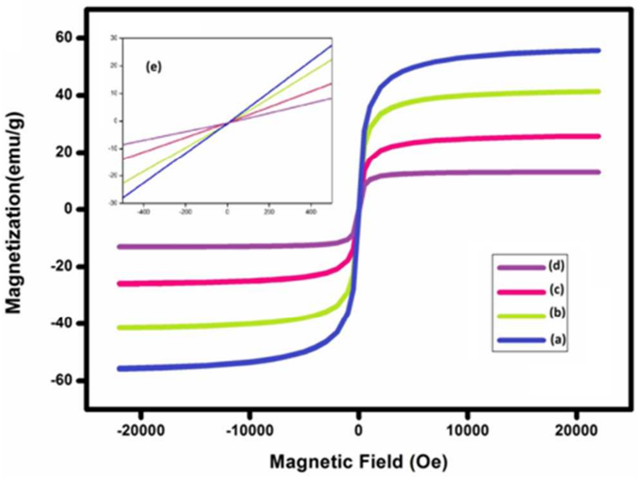

Fig. 6 Magnetization curves obtained by VSM at room temperature for (a) MNPs, (b) SMNPs, (c) ASMNPs, (d) Ni-TC@ASMNPs and (e) inset: enlarged image near the coercive field.

3.2 Catalytic studies

To investigate the catalytic efficacy of Ni-TC@ASMNPs and to determine optimal experimental conditions for Suzuki-Miyaura cross-coupling reaction, 4-bromoacetophenone and phenylboronic acid were chosen as model substrates and were treated under different temperature conditions, using various solvents and bases. To gain a better insight into the nature of prepared nickel nanocatalyst and its best source, various experiments were conducted without ligand, without PPh_3 and with different amount of nanocatalyst.

3.2.1 Catalytic activity of Ni-TC@ASMNP catalyst in Suzuki-Miyaura cross coupling reaction

As a starting point for optimizing Suzuki-Miyaura cross coupling reaction, the impact of various bases on the efficiency of this procedure was studied since its nature is known to be crucial in this type of coupling reaction. The highest yield was obtained when the reaction was carried out using K_3PO_4 as a base. However, when stronger alkalies (KO^{t}Bu or NaOH) were used, product was obtained in traces. Cs_2CO_3 and K_2CO_3 were also employed, and in both the cases low yields were obtained. Under various conditions, 100 °C was optimum temperature **(Fig. 7)** and 1, 4-dioxane was found to be the most effective solvent while the use of toluene, DMF and DMSO were inefficient for the reaction **(Fig. 8)**. Lower temperature resulted in prolonged reaction time for the complete conversion into the desired product and the yield was lower. Besides this, a control experiment without catalyst was conducted at 100 °C and no product was observed even after 24 h of reaction. Similarly, the use of Ni@ASMNPs and 20 mol% PPh_3 resulted in trace yield after 24 h. We also performed the reaction without phosphine as additive but obtained no product. Therefore, the addition of phosphine was essential, and PPh_3 gave desirable results. Finally, we performed the reaction with the synthesized catalyst Ni-TC@ASMNP with 20 mol% PPh_3 and found higher yield. This clearly indicated that, though the reaction is catalysed by metal, but, the role of ligand is equally important to carry out the transformation. In this case, the S, N-bidentate ligand with the strong σ donation acted as a co-catalyst and was effectively bound to the metal. The effect of catalyst loading was also investigated by employing different quantities of the catalyst **(Table 1, entries 3-7)**. A significant increase in the percentage yield of the product was observed when the amount of catalyst was increased from 5 to 10 mg. This suggests that the reaction rate depends on the Ni concentration.[4g] Since the role of transition metal in the coupling reaction is to provide an active site for the reaction to take place, rate of the reaction gets enhanced as number of active sites increases with the amount of the catalyst.[10] The best result was obtained with 15 mg of the catalyst.

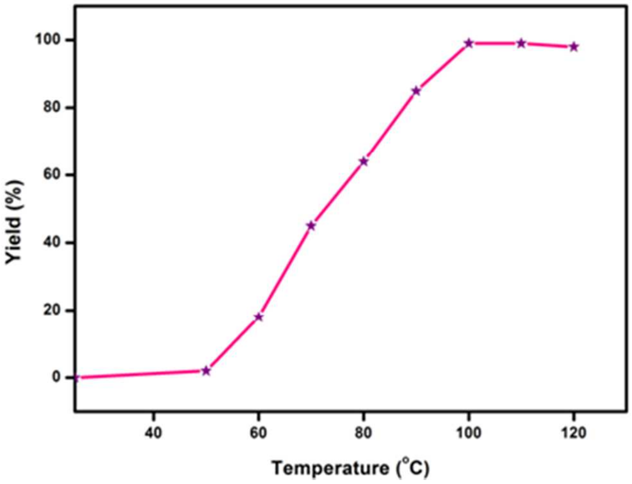

Fig. 7 Effect of temperature on model reaction for Suzuki-Miyaura cross-coupling reaction (Reaction conditions: 4-bromoacetophenone (0.5 mmol), phenylboronic acid (0.6 mmol), dioxane (1 mL), K_3PO_4 (0.75 mmol), catalyst (15 mg), PPh_3 (20 mol%), time (10 h)

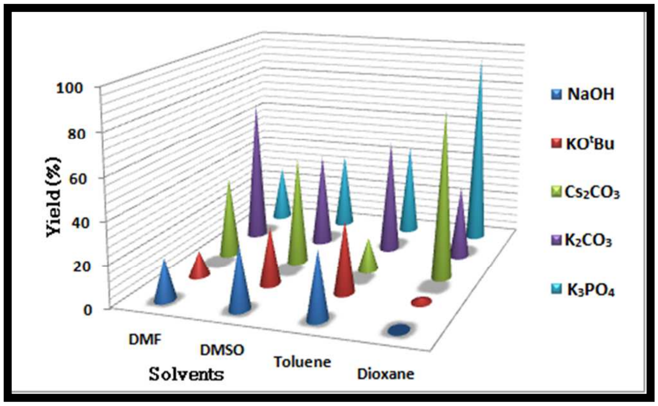

View Article Online
DOI: 10.1039/C4CY01736F

Fig. 8 Effect of bases and solvents on the catalytic efficiency of Ni-TC@ASMNP in Suzuki-Miyaura cross-coupling reaction (Reaction conditions: 4-bromoacetophenone (0.5 mmol), phenylboronic acid (0.6 mmol), solvent (1 mL), base (0.75 mmol), *Ni-TC@ASMNP* (15 mg), PPh_3 (20 mol%), time (10 h)

T**able 1** Screening of Nickel catalyst for Suzuki-Miyaura cross-coupling reaction[a]

Entry	Catalyst	Phosphine	Time (h)	Yield (%)[b]
1.	No	PPh_3	24	-
2.[c]	Ni@ASMNPs (20mg)	PPh_3	24	Trace
3.[d]	*Ni-TC@ASMNP* (5 mg)	PPh_3	10	Trace
4.[e]	*Ni-TC@ASMNP* (10 mg)	PPh_3	10	52
5.[f]	*Ni-TC@ASMNP* (15 mg)	PPh_3	10	94
6.[g]	*Ni-TC@ASMNP* (20 mg)	PPh_3	10	93
7.[*]	*Ni-TC@ASMNP* (15 mg)	-	10	-

[a] Reaction conditions: 4-bromoacetophenone (0.5 mmol), phenylboronic acid (0.6 mmol), dioxane (1 mL), K_3PO_4 (0.75 mmol), PPh_3 (20 mol%), time (10 h)

[b] Yield was determined by GC-MS

Amount of *Ni-TC@ASMNP*: c-20 mg, d-5 mg, e-10 mg, f-15 mg, g-20 mg

[*] Reaction performed without PPh_3

To investigate the generality of this cross-coupling reaction, we studied the reaction of phenylboronic acid with the range of aryl halides (Cl, Br, I) under the present optimized conditions. Regardless of their electronic characters, phenylboronic acid coupled smoothly with aryl bromides and iodides bearing both electron-deficient and electron-rich substituents, to afford the corresponding products in good to excellent yields with high turnover numbers (TON). It was also observed that the yield was lower in case of ortho- substituted aryl halides than those obtained with para-substituted ones, which might be due to steric factors. While aryl chlorides showed lower yields, which can be correlated with their poor reactivity toward oxidative addition in the catalytic cycle. In order to further explore the scope of the synthesized Nickel catalyst, we performed reaction of phenyl boronic acid with aryl tosylates, mesylate and heteroaryl halides. To our delight, all the substrates gave good to excellent yields for Suzuki-Miyaura cross coupling reaction. In case of tosylates and mesylate, excellent yields were obtained. It is also noteworthy that in case of heteroaryl halides, yields were found to be slightly lower. All reactions were performed on the same scale (0.5 mmol) and isolated yields of the products have been summarized in **Table 2**.

View Article Online
DOI: 10.1039/C4CY01736F

Cite this: DOI: 10.1039/c0xx00000x

www.rsc.org/xxxxxx

ARTICLE TYPE

Table 2. Suzuki- Miyaura cross-coupling reaction of phenyl boronic acid (1) with aryl halides (2) as per scheme 2 [a]

Entry	Boronic Acid	Aryl Halides/Tosylate/Mesylate	Product	Time (h)	Yield[b] (%)	TON[c]
1	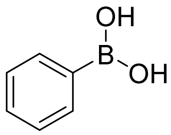 **1a**	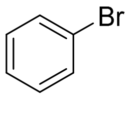 **2a**	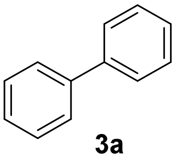 **3a**	10	93	298
2	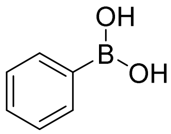 **1a**	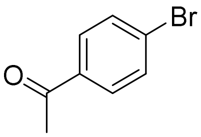 **2b**	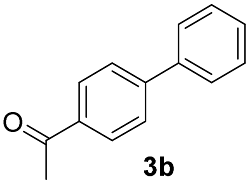 **3b**	10	94	301
3	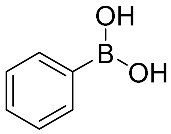 **1a**	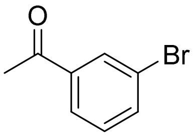 **2c**	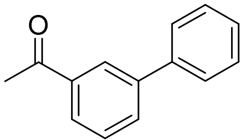 **3c**	10	94	301
4	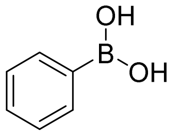 **1a**	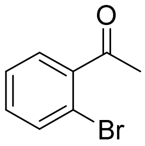 **2d**	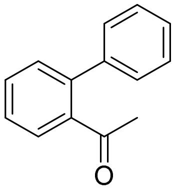 **3d**	10	85	272
5	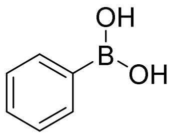 **1a**	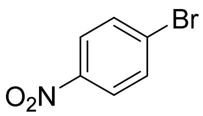 **2e**	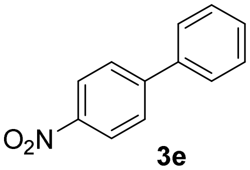 **3e**	10	95	304
6	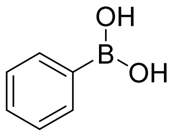 **1a**	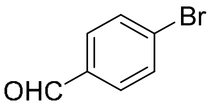 **2f**	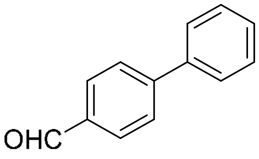 **3f**	10	91	291

View Article Online
DOI: 10.1039/C4CY01736F

7	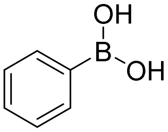 **1a**	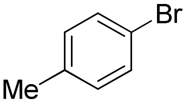 **2g**	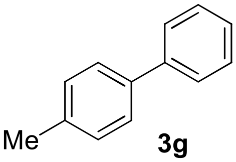 **3g**	11	87	278
8	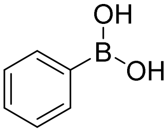 **1a**	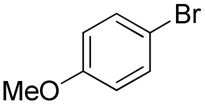 **2h**	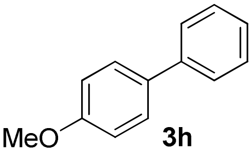 **3h**	11	87	278
9	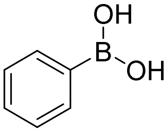 **1a**	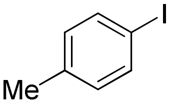 **2i**	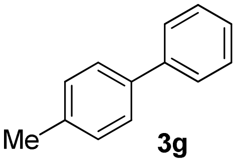 **3g**	10	92	294
10	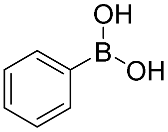 **1a**	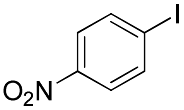 **2j**	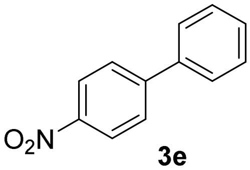 **3e**	10	98	314
11	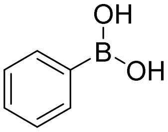 **1a**	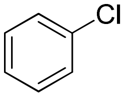 **2k**	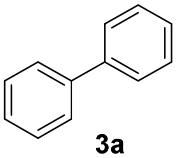 **3a**	12	83	266
12	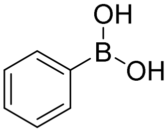 **1a**	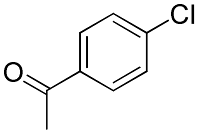 **2l**	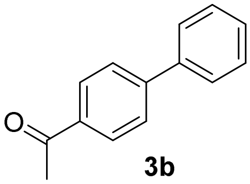 **3b**	12	86	275
13	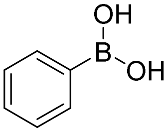 **1a**	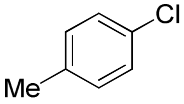 **2m**	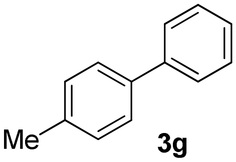 **3g**	13	77	246
14	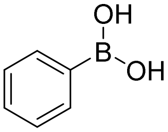 **1a**	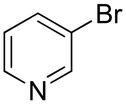 **2n**	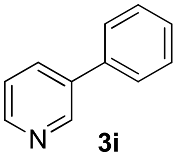 **3i**	10	75	240
15	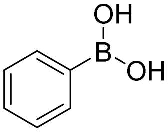 **1a**	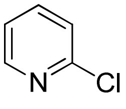 **2o**	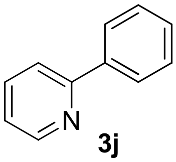 **3j**	15	78	250

View Article Online
DOI: 10.1039/C4CY01736F

16	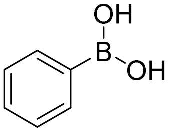 **1a**	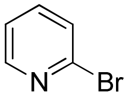 **2p**	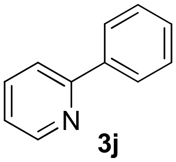 **3j**	10	82	263
17	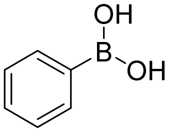 **1a**	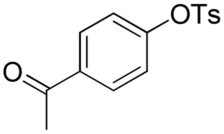 **2q**	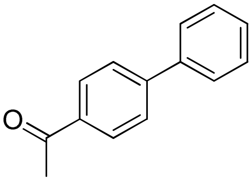 **3b**	10	97	310
18	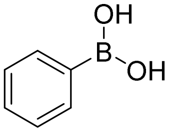 **1a**	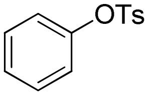 **2r**	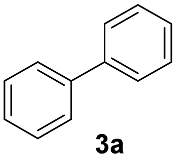 **3a**	10	89	285
19	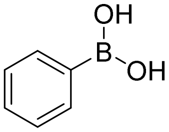 **1a**	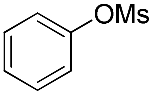 **2s**	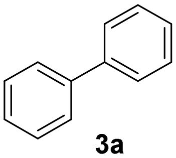 **3a**	10	81	259

[a] Reaction conditions: aryl halide (0.5 mmol), phenylboronic acid (0.6 mmol), dioxane (1mL), K_3PO_4 (0.75 mmol), Ni-TC@ASMNP (15 mg), PPh_3 (20 mol%),

[b] Yield was determined by GC-MS

[c] TON= Calculated using the 0.208 mmol/g Nickel (Obtained by AAS for Ni-TC@ASMNP)

Also, the present catalytic system was compared with previously reported catalysts (**Table 3**), and observed that our organic–inorganic hybrid catalytic system (Ni-TC@ASMNP) is much better than the literature precedents in terms of yield, cost, reaction time, stability, selectivity, turn over number, recovery and reusability. The high catalytic activity could be attributed to the high dispersion of nikel active sites onto the outer surface of the TC@ASMNP.

Table 3. Comparison of Ni-TC@ASMNP with literature precedents using Ni based homogeneous and heterogeneous catalysts for Suzuki-Miyaura cross coupling reaction

S.No	Boronic Acid	Aryl halide	Catalyst	Reaction conditions	Yield (%)	Ref.
1	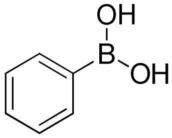	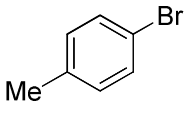	Ni(II) mounted on graphite (Ni/Cg)	K_3PO_4, PPh_3, LiBr, dioxane, 180-200 °C, 9h	87	10b
2	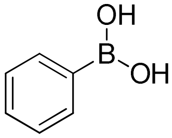	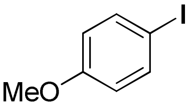	Magnetic Fe–Ni Alloy	NaOH, PCy_3, dioxane, 120 °C, 12h	95	11a

View Article Online
DOI: 10.1039/C4CY01736F

3	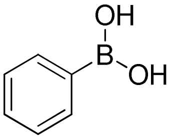	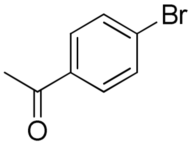	Monodisperse Ni and NiO nanoparticles	DMSO, 135 °C	98	11c
4	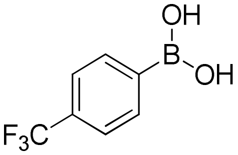	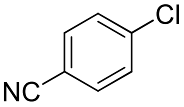	Nickel in charcoal (Ni/C)	KF, PPh_3, LiOH, MW, 180 °C, 30 min	91	10e
5	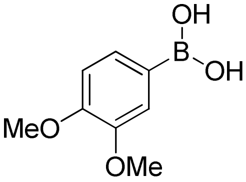	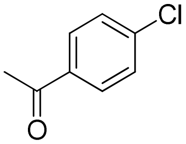	Ni(II)/Cg	PPh_3, K_3PO_4, dioxane, LiBr, 180 °C, 10 h	92	10d
6	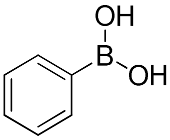	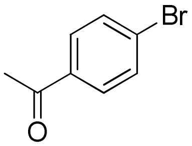	HPMC stabilized Ni Nanoparticles	Ethylene Glycol, Cs_2CO_3, 100 °C, 20 h	99	11b
7*	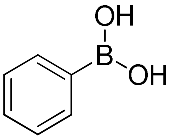	$BrCF_2COOEt$	$Ni(NO_3)_2.6H_2O$	dioxane, bpy, 60 °C, 24 h	95	7g
8*	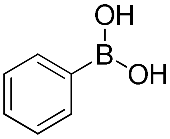	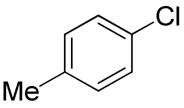	Ni(II) σ-aryl complex	PPh_3, K_2CO_3, toluene, 110 °C, 18 h	95	20a
9	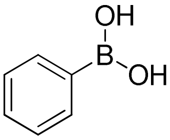	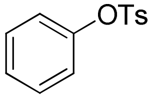	Bis-NHC pincer Ni complex	K_3PO_4, PPh_3, dioxane, 100 °C, 24 h	80	9b
10	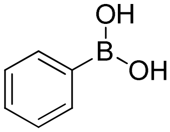	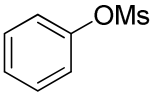	Bis-NHC pincer Ni complex	K_3PO_4, PPh_3, dioxane, 100 °C, 24 h	77	9b
11	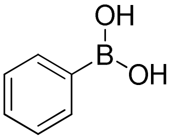	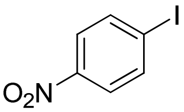	Ni-TC@ASMNP	K_3PO_4, PPh_3, dioxane, 100 °C, 10 h	98	Present work
12	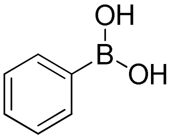	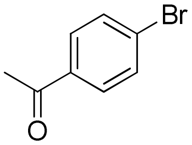	Ni-TC@ASMNP	K_3PO_4, PPh_3, dioxane, 100 °C, 10 h	94	Present work

View Article Online
DOI: 10.1039/C4CY01736F

---

* Homogeneous catalyst

3.2.2 Catalytic Stability & Reusability

A long life span and the ability to easily recover are highly desirable features of a catalyst for its industrial applications. In this regard, the recyclability of Ni-TC@ASMNP was investigated by using 4-Iodobenzene and phenylboronic acid as model substrates. The catalyst was smoothly separated using external magnet after the completion of the reaction and was washed with ethanol, dried under vacuum and reused in subsequent reactions. Nearly, quantitative catalyst could be well retrieved from each run. In a test of six cycles, the catalyst could be recovered without any substantial loss of catalytic activity **(Fig. 9)**. The recovered catalyst after six runs had no change in composition, attributing to EDS in comparison to the fresh one. Moreover, no morphological change was observed in TEM (See ESI-S4, S6) and SEM micrographs of the recovered catalyst. Furthermore, magnetism exhibited by the used nanocatalyst is sufficiently good for its effective separation from the reaction mixture via an external magnet **(Fig. 10)**.

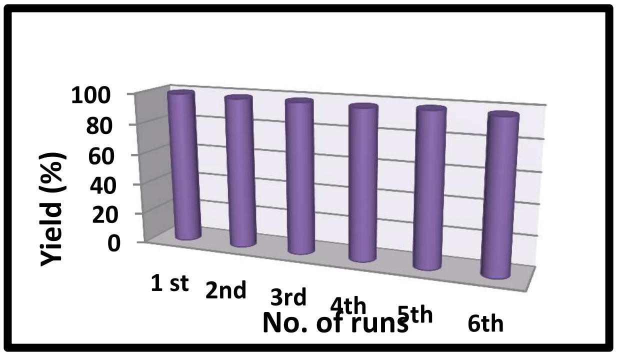

Fig. 9 Catalyst recycling test for successive six runs of Suzuki-Miyaura cross coupling reaction

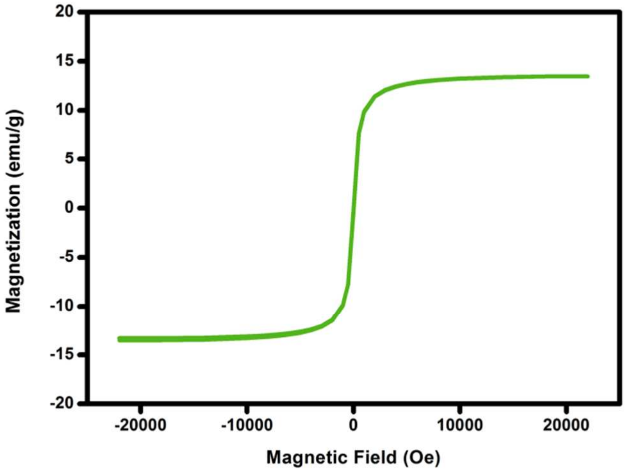

Fig.10 Magnetization curve obtained by VSM at room temperature for re-used Ni-TC@ASMNPs

3.2.3 Split test

While using a heterogeneous catalyst, there is a possibility of migration of the active species from solid support to the liquid phase, as the leached species become more liable for catalytic activity. Thus, to explore the catalyst leaching, a hot-filtration or split test was performed for desired reaction. After completion of the reaction, the solid catalyst was separated through an external magnet and the filtrate was analyzed through an atomic absorption spectrometer which showed negligible leaching. Again the standard reaction was conducted in the presence of the catalyst for 6 hours (70% conversion by GC), and then the catalyst was removed using a magnet and the reaction was carried further. No coupling product was detected even up to 10 hours in the reaction mixture under the same condition, thereby indicating truly heterogeneous nature of the magnetic nanocatalyst.

3.3 Proposed catalytic mechanism

The probable mechanism for Ni-TC@ASMNP catalyzed Suzuki-Miyaura cross coupling is illustrated in **Fig. 11**, which involves three sequential steps: oxidative addition, transmetalation and reductive elimination.[8a] The reaction starts with the in situ generation of active Ni(0) precatalyst prior to main catalytic cycle **(Fig. 11a)**.[22] We assume that the role of additional PPh_3 is to stabilize the active catalyst. Further, this Ni(0) species undergoes oxidative addition with aryl halide to yield Ni(II) σ-aryl complex **(Fig. 11b)** which contains a weakly coordinated halide ion. The transmetalation of the aryl group of the activated arylboronic acid

View Article Online
DOI: 10.1039/C4CY01736F

to Ni(II) σ-aryl complex gives Ni(II) diaryl complex **(Fig. 11c)**. Finally, reductive elimination of complex facilitates the catalytic cycle by regenerating the active Ni(0) species while the cross coupled product is produced **(Fig. 11d)**.

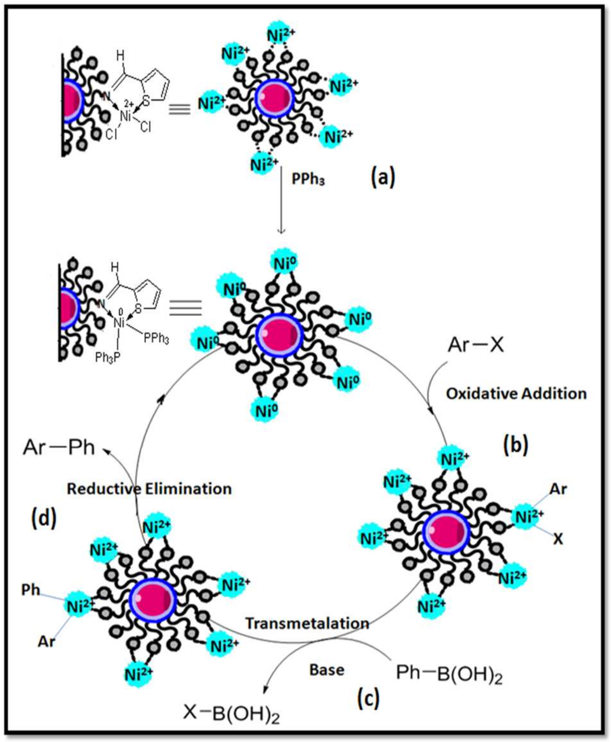

Fig. 11 Proposed catalytic mechanism for Ni-TC@ASMNP catalyzed Suzuki-Miyaura cross-coupling reaction

Conclusions

In conclusion, we have developed a highly selective, economical, and efficient silica based organic–inorganic hybrid Nickel nanocatalyst for Suzuki cross-coupling reaction. The targeted coupling reactions were achieved, under relatively mild experimental conditions and in reasonably high yield. Moreover, the catalyst is stable, shows negligible leaching and maintains high catalytic activity over six cycles. Follow-up studies directed at expanding the scope of this catalyst are underway. Additionally, facile synthetic procedure, broad substrate scope, short reaction time, high yield, effortless magnetic recovery and reusability for the reaction make it a favourable protocol from environmental and industrial view point.

Acknowledgements

One of the authors, Manavi Yadav thanks USIC, University of Delhi, Delhi, India and TERI, Gurgaon, India for providing instrumentation facilities.

Notes and references

[a] *Green Chemistry Network Centre, Department of Chemistry, University of Delhi, Delhi- 110007, India. Fax: +91-011-27666250; Tel: 011-27666250, E-mail: rksharmagreenchem@hotmail.com*
[b] *Biotechnology and Management of Bioresources Division, The Energy and Resources Institute, New Delhi-110003, India.*

† Electronic Supplementary Information (ESI) available: [details of any supplementary information available should be included here]. See DOI: 10.1039/b000000x/

1 (*a*) E. –i, Negishi, *Acc. Chem. Res.*, 1982, **15**, 340; (*b*) J. K. Stille, *Angew. Chem.*, 1986, **98**, 504; (*c*) J. K. Stille, *Angew. Chem. Int. Ed. Engl.*, 1986, **25**, 508; (*d*) R. F. Heck in Comprehensive Organic Synthesis, Vol. 4 (Eds.: B. M. Trost, I. Fleming), Pergamon, Oxford, 1991, p. 833; (*e*) N. Miyaura, A. Suzuki, *Chem. Rev.*, 1995, **95**, 2457; (*f*) V. Ritleng, C. Sirlin, M. Pfeffer *Chem. Rev.*, 2002, **102**, 1731; (*g*) D. R. Stuart, K. Fagnou, *Science.*, 2007, **316**, 1172.

2 (*a*) D. A. Horton, G. T. Bourne, M. L. Smythe, *Chem. Rev.*, 2003, **103**, 893; (*b*) G. Bringmann, C. Gunther, M. Ochse, O. Schupp, S. Tasler, Biaryls in Nature: A Multi-Faceted Class of Stereochemically, Biosynthetically, and Pharmacologically Intriguing Secondary Metabolites (Springer-Verlag, New York, 2001); (*c*) L. J. Gooßen, G. Deng, L. M. Levy, *Science.*, 2006, **313**, 662; (*d*) P. J. Hajduk, M. Bures, J. Praestgaard, S. W. Fesik, *J. Med. Chem.*, 2000, **43**, 3443; (*e*) G. W. Bemis, M. A. Murcko, *J. Med. Chem.*, 1996, **39**, 2887.

3 (*a*) Metal-Catalyzed Cross-Coupling Reactions (Eds.: F. Diederich, P. J. Stang), Wiley-VCH, New York, 1998; (*b*) T.-Y. Luh, M.-K. Leung, K.-T. Wong, *Chem. Rev.*, 2000, **100**, 3187.

4 (*a*) A. Suzuki, *Angew. Chem. Int. Ed.*, 2011, **50**, 6723; (*b*) C. C. C. J. Seechurn, M. O. Kitching, T. J. Colacot, V. Snieckus, *Angew. Chem. Int. Ed.*, 2012, **51**, 5062; (*c*) E.-i, Negishi, *Angew. Chem. Int. Ed.*, 2011, **50**, 6738; (*d*) N. Kambe, T. Iwasakia, J. Terao, *Chem. Soc. Rev.*, 2011, **40**, 4937; (*e*) C. M. So, F. Y. Kwong, *Chem. Soc. Rev.*, 2011, **40**, 4963; (*f*) M. –J. Jin, D. –H. Lee, *Angew. Chem. Int. Ed.*, 2010, **122**, 1137; (*g*) Y. Li, X. M. Hong, D. M. Collard, M. A. E.-Sayed, *Org. Lett.*, 2000, **2**, 2385.

5 J. R. Dodson, A. J. Hunt, H. L. Parker, Y. Yang, J. H. Clark, *Chem. Eng. Process.*, 2012, **51**, 69.

6 (*a*) R. Jana, T. P. Pathak, M. S. Sigman, *Chem. Rev.*, 2011, **111**, 1417; (*b*) L. Zhang, Z. Zuo, X. Leng, Z. Huang, *Angew. Chem. Int.*

View Article Online
DOI: 10.1039/C4CY01736F

Ed., 2014, **53**, 2696; (*c*) C. –T. Yang, Z.–Q. Zhang, Y. –C. Liu, L. Liu, *Angew. Chem. Int. Ed.*, 2011, **50**, 3904; (*d*) T. Hatakeyama, T. Hashimoto, K. K. A. D. S. Kathriarachchi, T. Zenmyo, H. Seike, M. Nakamura, *Angew. Chem. Int. Ed.*, 2012, **51**, 8834.

7 (*a*) F. G. –Bobes, G. C. Fu, *J. Am. Chem. Soc.*, 2006, **128**, 5360; (*b*) P. Leowanawat, N. Zhang, A. –M. Resmerita, B. M. Rosen, V. Percec, *J. Org. Chem.*, 2011, **76**, 9946; (*c*) C. E. I. Knappke, A. J. von Wangelin, *Angew. Chem. Int. Ed.*, 2010, **49**, 3568; (*d*) X. Hu, *Chem. Sci.*, 2011, **2**, 1867; (*e*) S. L. Zultanski, G. C. Fu, *J. Am. Chem. Soc.*, 2013, **135**, 624; (*f*) N. Zhang, D. J. Hoffman, N. Gutsche, J. Gupta, V. Percec, *J. Org. Chem.*, 2012, **77**, 5956; (*g*)Y. –L. Xian, W. –H. Guo, G. –Z. He, Q. Pan, X. Zhang, *Angew. Chem. Int. Ed*, 2014, **53**, 1.

8 (*a*) F.-S. Han, *Chem. Soc. Rev.*, 2013, **42**, 5270; (*b*) S. Z. Tasker, E. A. Standley, T. F. Jamison, *Nature*, 2014, **509**, 299; (*c*) S. Kotha, K. Lahiri, D. Kashinath, *Tetrahedron*, 2002, **58**, 9633.

9 (*a*) M. Xu, X. Li, Z. Sun, T. Tu, *Chem. Commun.*, 2013, **49**, 11539; (*b*) T. Tu, H. Mao, C. Herbert, M. Xua, K. H. Dotz, *Chem. Commun.*, 2010, **46**, 7796; (*c*) K. W. Quasdorf, X. Tian, N. K. Garg, *J. Am. Chem. Soc.*, 2008, **130**, 14422; (*d*) K. Inamoto, J. -i. Kuroda, E. Kwon, K. Hiroya, T. Doi, *J. Organomet. Chem.*, 2009, **694**, 389; (*e*) M. Baghbanzadeh, C. Pilger, C. O. Kappe, *J. Org. Chem.*, 2011, **76**, 1507; (*f*) D. Zim, V. R. Lando, J. Dupont, A. L. Monteiro, *Org. Lett.*, 2001, **3**, 3049.

10 (*a*) R. K. Sharma , A. Pandey, S. Gulati, *Polyhedron*, 2012, **45**, 86; (*b*) R. K. Sharma, A. Pandey, S. Gulati, *Appl. Catal., A.*, 2012, **431**, 33; (*c*) R. K. Sharma, S. Gulati, *J. Mol. Catal. A: Chem.*, 2012, **363**, 291; (*d*) R. K. Sharma, D. Rawat, *Inorg. Chem. Commun.*, 2012, **17**, 58; (*e*) R. K. Sharma, C. Sharma, *Catal. Commun.*, 2011, **12**, 327; (*f*) R. K. Sharma, C. Sharma, *J. Mol. Catal. A Gen.*, 2010, **332**, 53; (*g*) R. K. Sharma, S. Sharma, *Dalton Trans.*, 2014, **43**, 1292; (*h*) R. K. Sharma, S. Sharma, G. Gaba, *RSC Adv.*, 2014, **4**, 49198.

11 (*a*) B. H. Lipshutz, J. A. Sclafani, P. A. Blomgren, *Tetrahedron*, 2000, **56**, 2139; (*b*) B. H. Lipshutz, T. Butler, E. Swift, *Org. Lett.*, 2008, **10**, 697; (*c*) E. You, P. Li, L. Wang, *Synthesis*, 2006, 1465; (*d*) T. A. Butler, E. C. Swift, B. H. Lipshutz, *Org. Biomol. Chem.*, 2008, **6**, 19; (*e*) B. H. Lipshutz, B. A. Frieman, C. –T. Lee, A. Lower, D. M. Nihan, B. R. Taft, *Chem. Asian J.*, 2006, **1**, 417.

12 (*a*) R. Zhang, C. Miao, S. Wang, C. Xia, W. Sun, *ChemCatChem.*, 2013, **5**, 142; (*b*) D. Maity, Md. M. R. Mollicka, D. Mondal, B. Bhowmick, S. K. Neogi, A. Banerjee, S. Chattopadhyay, S. Bandyopadhyay, D. Chattopadhyay, *Carbohydr. Polym.*, 2013, **98**, 80; (*c*) J. Park, E. Kang, S. U. Son, H. M. Park, M. K. Lee, K. W. Kim, H, –J. Noh, J. –H. Park, C. J. Bae, J. –G. Park, T. Hyeon, *Adv. Mater.*, 2005, **17**, 429; (*d*) S. Paul, K. Pradhan, S. Ghosh, S. K. De, A. R. Dasa, *Adv. Synth. Catal.,* 2014, **356**, 1301.

13 (*a*) G. A. Sotiriou, A. M. Hirt, P. Y. Lozach, A. Teleki, F. Krumeich, S. E. Pratsinis, *Chem. Mater.*, 2011, **23**, 1985; (*b*) Y. Lien, T. M. Wu, *J. Colloid Interf. Sci.*, 2008, **326**, 517; (*c*) Y. Lu, Y. Yin, B. T. Mayers, Y. Xia, *Nano Lett.*, 2002, **2**, 183; (*d*) S. Kralj, M. Drofenik, D. Makovec, *J. Nanopart. Res.*, 2011, **13**, 2829.

14 (*a*) S. C. Tsang, C. H. Yu, X. Gao, K. Tam, *J. Phys. Chem. B*, 2006, **110**, 16914; (*b*) D. Niu, Y. Li, X. Qiao, L. Li, W. Zhao, H. Chen, Q. Zhao, Z. Mac, J. Shi, *Chem.Commun.*, 2008, **44**, 4463; (*c*) J. L. V. –Escoto, R. C. H. – Phillips, W. Lin, *Chem. Soc. Rev.*, 2012, **41**, 2673.

15 (*a*) R. K. Sharma, Y. Monga, *Appl. Catal., A*, 2013, **454**, 1; (*b*) R. K. Sharma, Y. Monga, A. Puri, *Catal. Commun.*, 2013, **35,** 110; (*c*) R. K. Sharma, Y. Monga, A. Puri, G. Gaba, *Green Chem.*, 2013, **15**, 2800; (*d*) R. K. Sharma, Y. Monga, A. Puri, *J. Mol. Catal. A: Chem.*, 2014, **393**, 84; (*e*) R. K. Sharma, S. Dutta and S. Sharma, *Dalton Trans.*, 2015, **44**, 1303.

16 (*a*) V. Polshettiwar, R. S. Varma, *Org. Biomol. Chem.*, 2009, **7**, 37; (*b*) Z. Zhang, F. Zhang, Q. Zhu, W. Zhao, B. Ma and Y. Ding, *J. Colloid Interf. Sci.*, 2011, **360**, 189.

17 (*a*) J. Zhu, J. He, X. Du, R. Lu, L. Huang, X. Ge, *Appl. Surf. Sci.*, 2011, **257**, 9056; (*b*) M. Kooti, M. Afshari, *Mater. Res. Bull.*, 2012, **47**, 3473; (*c*) M. Yamaura, R. L. Camilo, L. C. Sampaio, M. A. Macedo, M. Nakamurad, H. E. Toma, *J. Magn. Magn. Mater.*, 2004, **279**, 210; (*d*) M. M. Farahani, N. Tayyebi, *J. Mol. Catal. A: Chem.*, 2011, **348**, 83.

18 (*a*) R. Abu-reziq, H. Alper, D. S. Wang, M. L. Post, *J. Am. Chem. Soc.*, 2006, **128**, 5279; (*b*) Q. Zhang, H. Su, J. Luo, Y. Wei, *Green Chem.,* 2012, **14**, 201.

19 (*a*) D. E. -Quesada, J. M. -Robles, P. M. -Torres, E. R. z-Castellon, A. J. -Lopez, *Langmuir,* 2003, **19**, 4985; (*b*) M. C. Biesinger, L. W. M. Lau, A. R. Gerson, R. St. C. Smart, *Phys. Chem. Chem. Phys.*, 2012, **14**, 2434.

20 (*a*) S. Wang, Z. Zhang, B. Li, J. Li, *Catal. Sci. Technol.*, 2013, **3**, 2104; (*b*) J. Wang, S. Zheng, Y. Shao, J. Liu, Z. Xu, D. Zhu, *J. Colloid Interface Sci.,* 2010, **349**, 293.

21 (*a*) A. Hu, G. T. Yes, W. Lin, *J. Am. Chem. Soc.*, 2005, **127**, 12486; (*b*) R. G. Digigowa, J. –F. Dechézelles, H. Dietsch, I. Geissbühler, D. Vanhecke, C. Geers, A. M. Hirt, B. R. –Rutishauser, A. P. –Fink, *J. Magn. Magn. Mater.*, 2014, **362**, 72.

22 (*a*) X. Lei, K. A. Obregon, J. Alla, *Appl. Organomet. Chem.,* 2013, **27**, 419; (*b*) R. L. Jezorek, N. Zhang, P. Leowanawat, M. H. Bunner, N. Gutsche, A. K. R. Pesti, J. T. Olsen, V. Percec, *Org. Lett.*, 2014, **16**, 6326; (*c*) B.-T. Guan, Y.Wang, B.-J. Li, D.-G. Yu, Z.-J. Shi, *J. Am. Chem. Soc.*, 2008, **130**, 14468.